Clays and Clay Minerals, Vol. 34, No. 3, 338–345, 1986.

HYDROXY-Cu-VERMICULITE FORMED BY THE WEATHERING OF Fe-BIOTITES AT SALOBO, CARAJAS, BRAZIL

PHILIPPE ILDEFONSE,[1] ALAIN MANCEAU,[2] DOMINIQUE PROST,[1] AND MARIA CHRISTINA TOLEDO GROKE[3]

[1] Laboratoire de Pédologie, Université Paris 7, 2 place Jussieu 75251 Paris Cedex 05, France

[2] Laboratoire de Minéralogie-Cristallographie, UA 0-9, Universités Paris 6 et 7, 4 Place Jussieu 75230 Paris Cedex 05, and Laboratoire pour l'Utilisation du Rayonnement Electromagnétique (LURE) C.N.R.S., 91450 Orsay, France

[3] Instituto di Geosciencias, Universidad de Sao Paulo, Caixa Postal 20-899 CEP 1014 98 Sao Paulo, Brazil

Abstract—Weathering of a copper stratiform deposit (schist) at Salobo, Brazil, has produced two distinct Cu-bearing minerals from a biotite parent: vermiculite and a manganese oxide containing as much as 13% and 25% CuO, respectively. Manganiferous products were formed as the result of an interhorizon transfer of solutions through a fissure system. Thus, the structural orientation of the schists was a major factor in controlling the supergene concentration of Cu. The Cu-vermiculite formed by the weathering of Fe-biotite, although the unweathered biotites in the parent rocks were found to contain no copper, suggesting that Cu was supplied by weathering solutions. X-ray powder diffraction (XRD) and cation-exchange capacity data for the Cu-vermiculite differ from those of typical Mg-vermiculite and are similar to those of hydroxy-Al-vermiculite. A comparison of the XRD pattern of the Cu-vermiculite with that of a Cu-free vermiculite indicates that Cu atoms are located in interlayer sites. Cu probably occurs in a brucite-like layer. The position and structure of the Cu K-absorption spectrum suggest that the Cu is divalent and exists in 6-fold coordination.

Key Words—Cation-exchange capacity, Copper, Intergrade, Manganese oxide, Supergene enrichment, Vermiculite, Weathering.

Résumé—L'altération supergène des schistes du dépôt stratiforme de cuivre de Salobo (Brésil) a produit deux phases minérales porteuses de cuivre, associées aux biotites: une vermiculite et des oxydes de manganèse contenant respectivement de 13% à 25% de CuO. Les produits manganésifères résultent de transferts interhorizons d'ions en solution dans le système fissural. Aussi, l'orientation structurale des schistes est un facteur majeur qui contrôle l'accumulation supergène du cuivre. La vermiculite Cu se forme à partir de l'altération des biotites Fe de la roche saine. Les biotites saines, cependant, ne contiennent pas de cuivre ce qui suggère que cet élément est fourni par les solutions d'altération. Les données de la diffraction des rayons X et les mesures de la capacité d'échange de cations obtenues à partir de la vermiculite Cu diffèrent notablement de celles de vermiculite Mg classique. Par contre, elles sont proches de celles des vermiculites hydroxy-alumineuses, bien connues par ailleurs. La comparaison des spectres de diffraction de la vermiculite Cu avec ceux de la vermiculite non cuprifère de la base du profil montre que les atomes de Cu sont localisés en sites interfoliaires. La position et la structure des spectres d'absorption X au seuil K du cuivre suggèrent que les atomes de cuivre sont divalents et en position hexacoordonnée.

INTRODUCTION

In tropical countries, weathering commonly leads to residual lateritic concentrations of metallic elements. These accumulations have been extensively investigated, especially in connection with ore bodies of Fe, Al, and Ni (see, e.g., Nahon *et al.*, 1976; Boulangé and Bocquier, 1983; Trescases, 1975; Pelletier, 1976). Little work has been carried out, however, on the geochemical behavior of copper in these environments, except for the work of Bassett (1958) on Cu-vermiculites from Northern Rhodesia that were formed by the weathering of biotite. The present paper constitutes one of the first investigations of the Cu stratiform deposit at Salobo, Carajas, Brazil. This sedimentary deposit is weathered into a thick oxidized saprolite in which Cu has been concentrated (average copper content is 0.77 CuO) in non-sulfide minerals (Farias and Saueressing, 1984). The weathering of biotites from several environments has been studied by many authors, and Bisdom *et al.* (1982) described the general features of such processes. The present study was undertaken to determine the mineralogy, geochemistry, and crystal chemistry of the Cu-bearing minerals arising from the weathering of biotite in the Salobo deposit.

GEOLOGICAL AND PEDOLOGICAL SETTING

The Salobo copper deposit is in the Carajas mining district, Para State, about 50 km northwest of the large iron ore body at Serra dos Carajas, Brazil. A primary mineralization of bornite, chalcopyrite, and chalcocite

Table 1. Microprobe analyses and structural formulae of parent rock biotites (sample CAC27).[1]

SiO_2	33.38	33.09	32.61
Al_2O_3	14.46	14.16	13.76
TiO_2	0.76	0.77	1.04
FeO	32.62	32.73	30.47
MgO	6.30	5.87	5.42
K_2O	8.92	8.86	9.17
Total	96.51	95.48	92.47
Si	2.70	2.71	2.75
Al^{IV}	1.30	1.29	1.25
Al^{VI}	0.08	0.08	0.12
Ti	0.05	0.05	0.06
Fe^{2+}	2.21	2.24	2.15
Mg	0.76	0.72	0.68
K	0.92	0.93	0.98

[1] Calculated on the basis of $O_{10}(OH)_2$.

has been found in iron-rich schists containing variable amounts of amphibole, garnet, biotite, magnetite, quartz, and minor feldspar. This stratiform copper deposit was metamorphosed to the amphibolite facies and then retromorphosed to the greenschist facies (Martins *et al.*, 1982).

Samples were collected in an oblique tunnel dug into the oxidized saprolite of the vertically dipping schist. Distances from the entrance of the tunnel (i.e., the surface) are reported below:

Sample	CAC27	CAC25	CAC23	CAC21	CAC17	CAC7	CAC4
Distance (m)	39.80	38.30	31.70	26.70	19.70	5.60	3.00

Samples CAC27 and CAC25 are unweathered or weakly weathered schists, whereas the other samples are crumbly and intensively altered. They commonly show remnant structures of the parent rock. The oxidized saprolite is heterogeneous because of the heterogeneous nature of the parent rock. Thus, mica-rich and amphibole-rich layers are both present. Some samples contain abundant garnets. Amphibole and biotite commonly coexist in thick layers. The weathering of garnet and amphibole has produced iron oxyhydroxide pseudomorphs. Copper is present in these products but in lesser amounts (as much as 4.48% CuO) than in weathered biotite products (Prost *et al.*, 1986).

EXPERIMENTAL

Thin sections of samples consolidated in epoxy resins were examined under a petrological microscope. They were also analyzed with a Camebax electron microprobe using an Ortec EEDS II energy-dispersive X-ray spectrometer (EDX). Undisturbed samples were examined with a JEOL-JSM T20 scanning electron microscope (SEM). Minerals were separated by crushing and hand picking under a binocular microscope and were identified with a Philips PW1730 X-ray powder diffractometer (XRD) using CoKα or CuKα radiations (40 kV, 40 mA). Purified Cu-bearing minerals were also studied at the Cu K-absorption edge using the radiation of the DCI storage ring at LURE (France) operating at 1.72 GeV and about 200 mA. The beam was monochromatized by a Si (400) "channel-cut" single crystal which provided a spectral resolution of about 2 eV at the Cu K-adsorption edge. Additional experimental details were given by Calas *et al.* (1984).

RESULTS

Petrologic results

Parent biotite. In the fresh schist (samples CAC25 and CAC27), biotite layers, about 2 mm wide, alternate with amphibole. The biotite is well crystallized and occurs as tabular grains 300–400 μm long; the grains are green and pleochroic (green to yellowish green). This color is consistent with a high concentration of iron (as much as 32%, Table 1), as was reported by Deer *et al.* (1962). Structural formulae calculated on the basis of $O_{10}(OH)_2$ show that octahedral sheets contain principally Fe atoms, consistent with the composition of Fe-biotites (Foster, 1960). The sum of octrahedral cations per formula unit was found to be more than the 3 expected for a trioctahedral structure because all iron was expressed as Fe^{2+}. Potassium is the common interlayer cation; its concentration corresponds to the standard layer charge of mica. Some microprobe analyses of these two samples showed low concentrations of K_2O, incompatible with true micas; however, these biotites displayed no weathering features by optical examination, suggesting that weathering in these samples was in an early stage. The bulk rock appeared unweathered. No copper was detected in these parent biotites.

Weathered biotite. In the oxidized schist (saprolite), secondary products were noted pseudomorphous after biotite. Exfoliation was also observed, especially at the boundaries of crystals (Figure 1-1). Pleochroism and color decreased in intensity compared with fresh biotites, as was also observed by Bisdom *et al.* (1982). Interlamellar voids were noted filled with reddish-brown, colorless, or black products. The black products were present only in weathered biotites where transmineral fissures (i.e., fissures traversing the rock) were parallel to 001 cleavages. In areas where fissures were perpendicular to cleavages, these alteration products were encountered only in the larger fissure systems (Figures 1-2 and 1-3). SEM investigation and EDX data suggest that exsolved iron recrystallized as ferruginous granules at the boundaries of crystals (Figure 1-4). Lamellae of weathered biotites were microfragmented but retained their original orientation.

Microprobe analyses of weathered biotites showed the chemical compositions to be dominated by Al and Fe. The Mg contents were either very low or similar to those of the fresh biotites (Table 2). Table 2 also shows that Fe and K were the most mobile ions during

https://doi.org/10.1346/CCMN.1986.0340315 Published online by Cambridge University Press

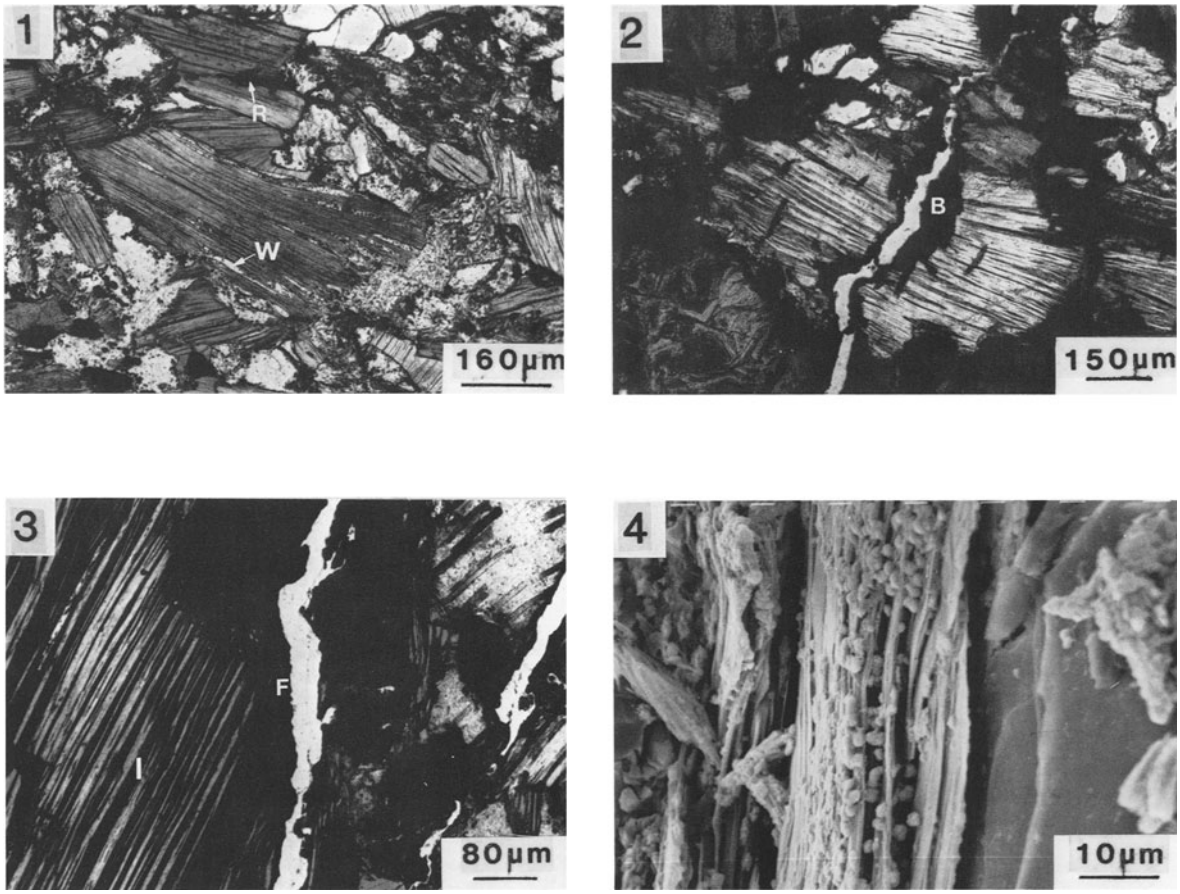

Figure 1. Microscopic features of weathered biotites. (1) Photomicrograph showing pseudomorphic transformation accompanied by exfoliated habitus. Colorless kaolin-like minerals (W) and reddish-brown product (R) in interlamellar voids (sample CAC21). (2) Photomicrograph showing transmineral fissure perpendicular to biotite cleavages containing Mn-Cu products (B) (natural light). (3) Photomicrograph showing black products in interlamellar voids (I) and in large fissures (F) where fissure system is parallel or subparallel to cleavage planes of weathered mica (natural light). (4) Scanning electron micrograph showing excluded iron phases at the boundaries of clay flakes.

weathering. The presence of different amounts of Cu is also significant. The most highly altered minerals were observed in the deepest levels of the weathered zone (with the exception of sample CAC23), nevertheless the Cu concentration was high even in the upper horizons. Large variations in the Cu concentrations appeared to follow those of Fe and Mg (Figure 2). On the other hand, Cu and K were negatively correlated; i.e., the more weathered the biotite, the richer in Cu were its secondary products (Figure 3).

The geochemical characterization of interlamellar secondary minerals suggests that the reddish-brown products are rich in Fe and contain little Cu (Table 3). The colorless minerals have a Si/Al ratio of about 1 (Table 3) and exhibit a tubular habit under the SEM, similar to that of some kaolin-group minerals (Keller, 1977). The black products in the upper part of the tunnel (samples CAC4 and CAC7) (Table 3) are very rich in Mn and Cu (as much as 25% CuO). Similar products were also observed in voids of garnet pseudomorphs and inside large transmineral fissures (Prost *et al.*, 1986).

TEM investigations were made of separated Cu-biotites, after the samples were ground and dispersed by ultrasonic treatment, to determine whether Cu atoms were actually associated on a micrometer scale with a phyllosilicate or contained in a separate phase, e.g., chrysocolla (Van Oosterwyck-Gastuche, 1970). TEM observations and EDX analyses showed only flat or planar Cu-bearing flakes. On this scale, Cu always appeared to be associated with Si, Al, Fe, and K. Chemical analyses of weathered biotites indicate that the phyllosilicates acted as a major host for Cu in the oxidized saprolite of the weathered schist.

X-ray powder diffraction results

XRD patterns of the purified sandy fraction (samples CAC23 and CAC4, 300–400 µm) gave the reflections

https://doi.org/10.1346/CCMN.1986.0340315 Published online by Cambridge University Press

Table 2. Microprobe analyses of weathered biotites.[1]

Sample	SiO_2	Al_2O_3	TiO_2	FeO	MnO	MgO	CuO	K_2O	Total
CAC23	40.63	26.14	0.46	14.10	0.17	0.50	0.27	4.44	86.71
	36.74	21.21	1.08	12.38	0.93	0.77	0.38	4.12	77.60
	33.28	20.14	0.84	13.71	1.30	1.41	0.55	3.72	74.95
	34.97	19.55	1.04	15.71	1.31	1.85	0.47	4.57	79.47
CAC21	34.48	20.75	1.83	19.85	—	2.09	6.76	1.68	87.44
	27.95	12.59	2.30	26.11	—	2.80	10.33	1.15	83.23
	28.74	13.24	2.62	26.27	—	3.25	13.20	0.88	88.20
CAC17	29.90	14.02	2.01	24.66	—	2.91	11.55	2.47	87.52
	32.85	14.14	1.47	26.09	—	4.05	6.09	4.83	89.52
	30.99	13.65	1.65	27.81	—	4.53	6.49	4.16	89.28
	28.33	11.97	1.47	30.77	—	5.50	3.34	4.10	85.48
	31.65	13.78	1.64	23.88	—	6.01	11.13	2.18	90.27
CAC7	32.97	18.81	1.21	16.06	0.42	3.04	5.12	2.32	79.95
	28.56	12.39	1.40	18.95	—	3.83	7.31	3.33	75.77
	31.58	13.36	1.57	22.76	0.39	3.93	5.48	5.44	84.51
	27.89	11.94	1.57	19.73	—	4.02	6.46	2.72	74.33
	30.48	12.91	1.28	23.57	0.26	4.04	6.87	4.52	83.93
	28.46	14.37	3.01	18.64	1.19	4.13	6.04	1.84	77.68
	29.08	12.43	1.41	23.29	—	4.13	6.59	3.96	80.89
CAC4	29.13	11.10	0.42	28.66	—	5.05	5.46	5.21	85.03
	32.85	14.38	1.48	24.20	—	5.55	6.41	4.99	89.86
	30.19	11.79	0.44	26.87	—	5.69	5.77	5.32	86.07
	29.82	12.52	1.74	24.82	1.05	5.83	10.40	2.57	88.75
	30.05	12.06	1.69	22.86	0.36	5.85	9.58	2.15	84.60
	31.19	12.49	1.31	24.50	—	5.90	6.13	5.20	86.72
	32.79	13.35	1.57	25.69	—	6.41	6.24	4.95	91.00

[1] Total iron expressed as FeO.

of residual mica at 10.02 and 3.36 Å. The XRD pattern of sample CAC23 contained shoulders on the small angle side of these reflections; these reflections were weak in the XRD pattern of sample CAC4 (Figure 4). XRD patterns exhibited reflections at 14.14–14.16, 7.11–7.14, 4.74–4.75, 3.56, 2.85, and 2.01–2.02 Å, which may be attributed to vermiculite or chlorite or both. In sample CAC4, XRD peaks at 11.70, 8.20, 5.98, 4.84, and 3.45 Å correspond to a regular interstratification of biotite and a 14-Å mineral.

These minerals did not expand with ethylene glycol. After heating the sample to 600°C, a single reflection persisted at 10.16 Å, however, mild heating at 200°, 300°, and 450°C partially collapsed the layers (Figure 5). A reflection at 11.93 Å persisted as high as 300°C. The layers began to collapse to about 10.7 Å at 450°C. Similarly, the 003 reflection at 8.15 Å of the mixed-layer mineral did not collapse at temperatures less than 450°C. Such behavior is similar to that of the hydroxy-Al-vermiculite found in acid weathering materials and soils at pHs of 4–4.5 (Jackson, 1963; Tardy and Gac, 1968). Therefore, the biotite in sample CAC4 weathered to a complex assemblage of an intergrade vermiculite on the one hand and a mica/intergrade vermiculite mixed-layer phase on the other. The nature of the polymorph was determined from the relative intensity of the 201 reflections at 2.61 and 2.39 Å. The interlayer structure had the I_a polytype structure typical of Mg-vermiculites (Shirozu and Bailey, 1966). The exchange capacity, measured by displacement of exchangeable cations by ammonium ions, was 15–25 meq/100 g, whereas for typical Mg-vermiculite, it is as high as 150 meq/100 g (Foster, 1963). Thus, most of the interlayer cations were not exchangeable, consistent with the heating behavior which was also clearly different from that of a typical Mg-vermiculite. Important differences in basal-plane intensities were noted for the two samples (Figure 4). In sample CAC4, the 002, 003, and 007 reflections were enhanced, compared with the 001 reflection.

Petruk (1964) established that the intensity of the X-ray beam diffracted by even-order basal planes of chlorites increases with the content of heavy metals in octahedral layers. Therefore, the inversion of the relative intensities of the 001 and 002 reflections of samples CAC4 and CAC23 is probably due to the incorporation of Cu atoms in the structure of the hydroxy-vermiculite. In the same way, Brindley and Gillery (1956) and Petruk (1964) demonstrated that intensities of X-rays diffracted by odd-order planes are related to the distribution of the heavy atoms between octahedral sheets. In chlorite, where heavy atoms prevailed in the brucitic layer, the 001 and 005 intensities decreased, whereas the intensities of the 003 and 007 reflections increased. In sample CAC4, similar trends were noted, especially for the 001, 003, and 007 reflections, meaning that heavy atoms such as Cu were present in the interlayer position. Bassett (1958) came

https://doi.org/10.1346/CCMN.1986.0340315 Published online by Cambridge University Press

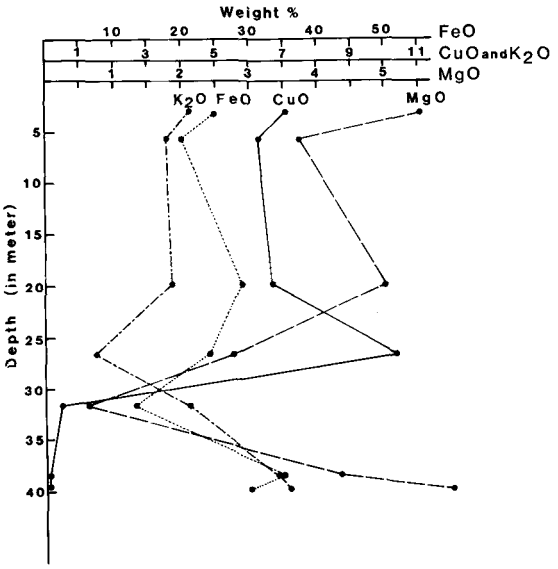

Figure 2. Variation of K_2O, MgO, FeO, and CuO contents of biotites throughout the weathering profile (wt. %).

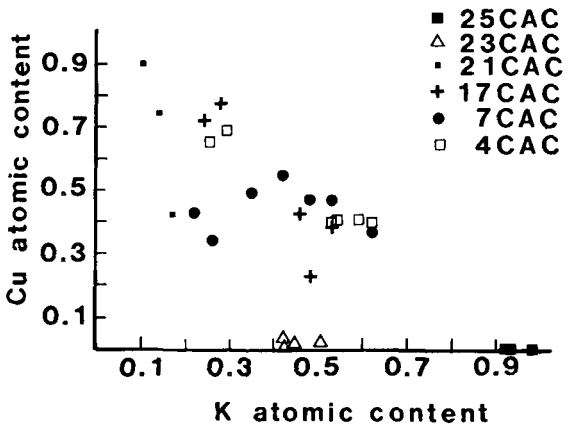

Figure 3. Correlation of Cu and K in weathered biotites throughout the weathering profile (atom contents on a $O_{10}(OH)_2$ basis).

to the same conclusion on the basis of 002 intensities. Petruk (1964) used the ratio I_{003}/I_{005} to quantify the "degree of assymetry," which is the number of heavy atoms in the mica-like layer less the number of heavy atoms in the brucite-like layer. For sample CAC23, the ratio I_{003}/I_{005} was near 1, whereas for sample CAC4, it was as much as 2 (Figure 6). The difference in the ratio of I_{003}/I_{005} was small because these minerals initially contained heavy atoms (Fe) in octahedral sites of the mica-like layer; this small shift corresponds to a relatively minor introduction of heavy atoms into octahedral sites of the brucite-like layer. Microprobe data have shown that the Cu content of sample CAC4 is much greater than that of sample CAC23. Thus, from XRD data, Cu probably entered interlayer sites.

K-edge spectroscopic results

The K-edge spectroscopic investigation was undertaken to determine the oxidation state and the coordination number of Cu. As is firmly established in the literature, the K-edge structure yields information about the electronic configuration of the element under study (see, e.g., the review by Calas *et al.*, 1984). The K-edge spectrum of Cu in vermiculite is displayed in Figure 7 along with those of Cu_2O and $Cu(OH)_2$, taken as Cu^+ and Cu^{2+} model compounds. The spectra of the phyllosilicate and $Cu(OH)_2$ differ from that of Cu_2O by their energy position and their structure. The energy of the main part of the absorption edge depends on the oxidation state and the degree of covalency. In the present study, only minerals in which Cu is coordinated with oxygen were examined to eliminate, as much as possible, the effect of covalency on the edge energy. The shift to higher energies observed between Cu_2O and $Cu(OH)_2$ is of about the same magnitude as that known for Cu^+ and Cu^{2+} in spinels (Hannoyer *et al.*, 1982).

The energy position of the K-edge of Cu in vermiculite indicates that the copper atoms were divalent. This oxidation state was confirmed by the structure of the edge. The Cu^+ spectrum contains a well-resolved feature on the steeply increasing slope of the absorption edge, a feature that has often been attributed to the 1s → 4s transition, whereas the Cu^{2+} spectrum shows

Table 3. Microprobe analyses of interlamellar products (sample CAC4).[1]

	Colorless product			Red product		Black product	
SiO_2	48.34	36.77	44.92	5.06	5.63	0.54	0.51
Al_2O_3	34.52	24.98	33.24	5.03	1.95	0.46	0.34
TiO_2	—	0.75	0.27	—	—	0.53	0.49
FeO	5.92	10.34	4.98	69.76	71.68	0.29	—
MnO	—	0.58	0.60	0.82	0.59	62.39	69.72
MgO	—	1.35	0.81	—	—	—	0.34
CuO	0.83	2.45	1.22	1.51	1.24	24.26	21.38
K_2O	0.24	1.80	1.20	—	—	0.35	0.27
Total	89.85	79.02	87.27	82.13	81.09	88.82	93.05

[1] Total iron expressed as FeO.

https://doi.org/10.1346/CCMN.1986.0340315 Published online by Cambridge University Press

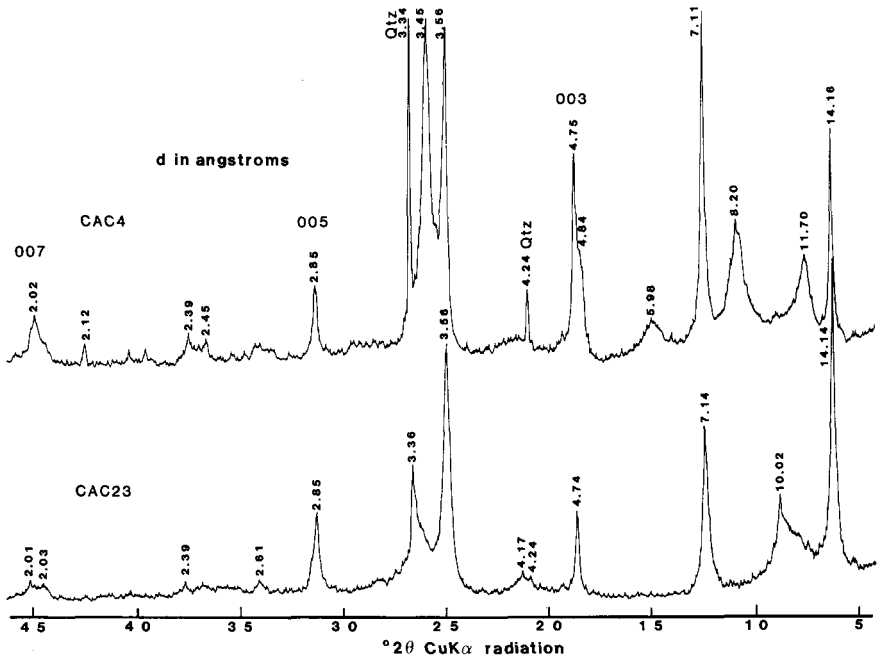

Figure 4. X-ray powder diffraction patterns of randomly oriented particles of weathered biotites from samples CAC23 and CAC4 (300–400 μm) (CuKα radiation).

three weak shoulders. The first shoulder (particularly weak) was observed at a lower energy than the main absorption peak and corresponds to a 1s → 3d state transition. This transition was not noted for Cu^+ which has no empty 3d sites ($3d^{10}$ configuration). Absorption features on the upslope and crest of the edge involved electronic processes which are not well understood. The feature at about 8 eV below the edge crest is presently assigned to the 1s → 4s or 1s → 4p plus "shake-down" transition (Bair and Goddard, 1980). The apex of the edge corresponding to the strong allowed 1s → 4p transition is split into two components. This split has classically been related to the lower symmetry of the site.

The structure of the edge also permits discussion of the coordination number. The influence of this parameter on the edge shape has been investigated in Cu-spinels having various degrees of inversion (Hannoyer *et al.*, 1982). The dipole-allowed transition from the 1s-core to the 4p-final-state transition yielded a sharp absorption feature (white line) in a 6-fold site, whereas in a 4-fold coordination the absorption above the edge crest remained high. Because the width of the edge crest in vermiculite was similar to that in $Cu(OH)_2$, evidence for a 4-fold Cu^{2+} was not obtained.

DISCUSSION

Many investigations have been devoted to the weathering of biotites. At Salobo, the present petrologic studies indicate that the phyllosilicates acted as a major host for Cu in the oxidized saprolite of the weathered schist. Interlamellar reddish-brown products were found to be ferruginous compounds that formed by the accumulation of Fe after intracrystalline transfer (as defined by Nahon and Bocquier, 1983) from weathered biotite layers towards interlamellar voids. Both high chemical discontinuity and petrologic relations with phyllosilicate layers indicate that the black products resulted from an interhorizon transfer by means of solution through fissure systems (i.e., absolute accumulation), independent of the weathering of the biotites. Mn came from the weathering of garnets which originally contained as much as 2.75% MnO.

Vermiculitization has often been described in soils and weathered rocks in temperate-climate countries (Walker, 1949; Novikoff *et al.*, 1972; Wilson, 1966, 1970); it has also been realized experimentally in the laboratory (Barshad, 1948; Newman and Brown, 1966; Robert, 1971). From these studies, it is well established that K is released during the biotite-vermiculite transformation; Mg and Fe are partially released; Mg is transferred to interfoliar sites; and Fe is oxidized and partially exsolved (Wey *et al.*, 1966). At Salobo, vermiculitization in the lateritic profile took place by weathering of Fe-biotite and was accompanied by the above processes at the bottom of the oxidized profile. In the upper part of the saprolite, however, the vermiculite-like minerals possess unusual chemical properties and XRD features, compared with typical vermiculite. The XRD data indicate that this material is

https://doi.org/10.1346/CCMN.1986.0340315 Published online by Cambridge University Press

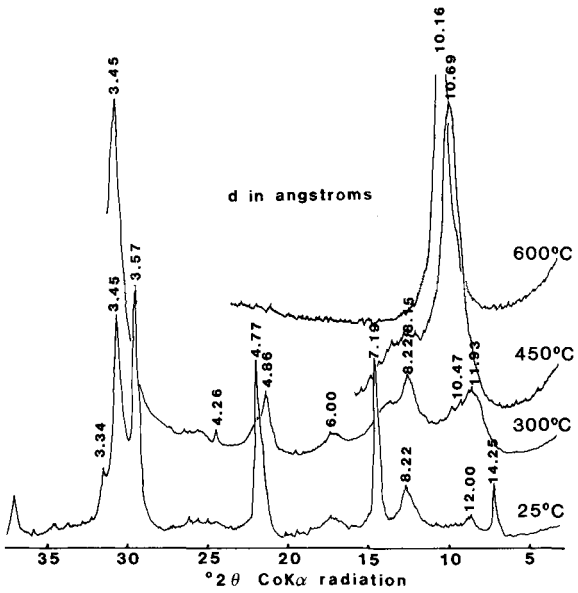

Figure 5. X-ray powder diffraction patterns of the 300–400-μm fraction of oriented particles of weathered biotite from sample CAC4 after heat treatment (CoKα radiation).

a Cu-bearing phyllosilicate. Copper atoms were apparently incorporated into the vermiculite during its formation from biotite and probably account for the peculiar XRD and chemical behavior of this mineral which is closely related to that of hydroxy-Al-vermiculite.

The foregoing results lend credence to the interlayer

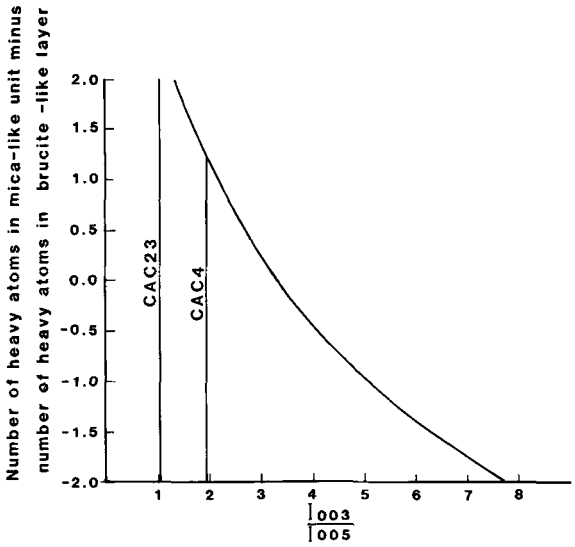

Figure 6. Relationship between number of heavy atoms in mica-like octahedral layer less number of heavy atoms in brucite-like layer and the I_{003}/I_{005} ratio in chlorites (after Petruk, 1964).

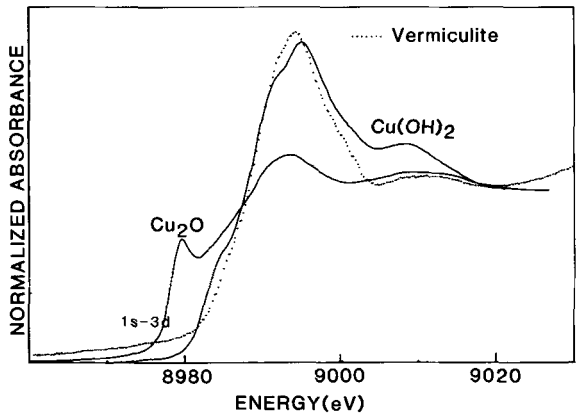

Figure 7. K-edge absorption spectra of Cu normalized by the "jump" at the edge.

location of Cu and suggest a partial chloritization, a feature that characterizes an intergrade mineral for which the interlayer sheet is an incomplete brucitic sheet. Indeed, the Si and Al content do not appear to have changed during the biotite-to-vermiculite transformation, which indicates that the tetrahedral sheets were not affected by weathering. Mg was less released than from non-Cu-bearing vermiculite, and no positive chemical correlation was found between Mg and Cu. On the other hand, no report has been found in the literature that suggests that Mg and Fe lead to intergrade minerals during the weathering of biotite. A Cu-vermiculite was described in Northern Rhodesia by Bassett (1958), but he did not report its intergrade properties, although he did note the possibility of Cu being largely surrounded by OH, rather than H_2O.

It is well known that vermiculite can sorb Al released during weathering into its interlayer space (Rich, 1968). This mechanism explains the existence of "chloritized" vermiculite in many weathering profiles. Such a mechanism is also possible for Cu, but the presence of light atoms, such as Mg, seems to be necessary to build small islands of a brucitic network, because $Cu(OH)_2$ possesses a lepidocrocite structure (as a result of the Jahn-Teller effect; Burns, 1970), not a brucite structure. The sorption of Cu by vermiculite appears to be an effective supergenic trap under oxidizing and acidic (pH < 6) conditions (Garrels and Christ, 1967), but ore enrichment is limited by the inability of Cu to form a pure Cu-brucite-type sheet.

ACKNOWLEDGMENTS

The authors thank A. J. Melfi and J. C Parisot for providing samples, M. Robert for access to XRD, cation-exchange measurements, and helpful comments, and the staff of LURE for synchroton facilities. This paper was improved by the constructive comments of J. Petiau, G. Bocquier, and G. Calas.

REFERENCES

Bair, R. A. and Goddard, W. A. (1980) *Ab initio* studies of the X-ray absorption edge in copper complexes: I. Atomic Cu^{2+} and Cu(II)Cl_2: *Phys. Review B.* **22,** 2767–2776.

Barshad, I. (1948) Vermiculite and its relation to biotite as revealed by exchange reactions, X-ray analysis, differential thermal curves, and water content: *Amer. Mineral.* **33,** 655–678.

Bassett, W. A. (1958) Copper vermiculites from Northern Rhodesia: *Amer. Mineral.* **43,** 1112–1133.

Bisdom, E. B. A., Stoops, G., Delvigne, J., Curmi, P., and Altemuller, H. J. (1982) Micromorphology of weathering biotite and its secondary products: *Pédologie* **32,** 225–252.

Boulangé, B. and Bocquier, G. (1983) Le rôle du fer dans la formation des pisolites alumineux au sein des cuirasses bauxitiques latéritiques: *Sci. Géol. Bull.* **72,** 29–36.

Brindley, G. W. and Gillery, F. H. (1956) X-ray identification of chlorite species: *Amer. Mineral.* **41,** 169–186.

Burns, R. G. (1970) *Mineralogical Application of Crystal Field Theory:* Cambridge University Press, Cambridge, 224 pp.

Calas, G., Bassett, W. A., Petiau, J., Steinberg, M., Tchoubar, D., and Zarka, A. (1984) Some mineralogical applications of synchrotron radiation: *Phys. Chem. Miner.* **11,** 17–36.

Deer, W. A., Howie, R. A., and Zussman, J. (1962) *Rock Forming Minerals: Vol. 3. Sheet Silicates:* Longmans, London, 270 pp.

Farias, N. F. and Saueressing, R. (1984) Jazida de cobre do Salobo 3A. *Anais I Simposio de Geologia da Amazonia, Belem,* 63–73.

Foster, M. D. (1960) Interpretation of the composition of trioctahedral micas: *U.S. Geol. Surv. Prof. Pap.* **354B,** 49 pp.

Foster, M. D. (1963) Interpretation of the composition of vermiculites and hydrobiotites: in *Clays and Clay Minerals, Proc. 10th Natl. Conf., Austin, Texas, 1961,* Ada Swineford and P. C. Franks, eds., Pergamon Press, New York, 70–89.

Garrels, R. M. and Christ, C. L. (1967) Equilibre des minéraux et de leurs solutions aqueuses: in *Monographies de Chimie Minérale,* Gauthier-Villars, Paris, 335 pp.

Hannoyer, B., Durr, J., Calas, G., Petiau, J., and Lenglet, M. (1982) Caractérisation d'oxydes de cuivre par spectrométrie d'absorption X: *Mater. Res. Bull.* **17,** 435–442.

Jackson, M. L. (1963) Interlayering of expansible layer silicates in soils by chemical weathering: in *Clays and Clay Minerals, Proc. 11th Natl. Conf., Ottawa, Ontario, 1962,* Ada Swineford, ed., Pergamon Press, New York, 29–46.

Keller, W. D. (1977) Scan electron micrographs of kaolins collected from diverse environments of origin. IV. Georgia kaolin and kaolinizing source rocks: *Clays & Clay Minerals* **25,** 311–345.

Martins, L. P. B., Saveressing, R., and Melo Vieira, M. A. (1982) Aspectos petrographicos das principais litologias da sequencia Salobo: *Anais do I Symposio de Geologia da Amazonia, Belem,* 253–262.

Nahon, D., Janot, C., Karpoff, A. M., Paquet, H., and Tardy, Y. (1976) Mineralogy, petrography and structures of iron crusts (ferricretes) developed on sandstones in the western part of Senegal: *Geoderma* **19,** 263–277.

Nahon, D. and Bocquier, G. (1983) Petrology of element transfers in weathering and soil systems: *Sci. Géol. Mém.* **72,** 111–119.

Newman, A. C. D. and Brown, G. (1966) Chemical changes during the alteration of micas: *Clay Miner.* **6,** 297–309.

Novikoff, A., Tsawlassou, G., Gac, J. Y., Bourgeat, F., and Tardy, Y. (1972) Altération des biotites dans les arènes des pays tempérés, tropicaux et équatoriaux: *Sci. Géol. Bull.* **25,** 287–305.

Pelletier, B. (1983) Localisation du nickel dans les minerais garniéritiques de Nouvelle-Calédonie: *Sci. Géol. Mém.* **73,** 173–183.

Petruk, W. (1964) Determination of the heavy atom content in chlorite by means of the X-ray diffractometer: *Amer. Mineral.* **49,** 61–71.

Prost, D., Ildefonse, P., Groke, M. C. T., Melfi, A. J., Delvigne, J., and Parisot, J. C. (1984) Alteraçao dos minerais na zona supergena da formaçao cuprifera do Salobo 3A (Serra dos Carajas). Localizaçao do cobre nos produtos secundarios: *Proc. Simposio de Geologia 33th,* Rio de Janeiro (in press).

Rich, C. I. (1968) Hydroxy-interlayers in expansible layer silicates: *Clays & Clay Minerals* **16,** 15–30.

Robert, M. (1971) Etude expérimentale de l'évolution des micas (biotites). I. Les processus de vermiculitisation: *Ann. Agron.* **22,** 43–93.

Shirozu, H. and Bailey, S. W. (1966) Crystal structure of a two-layer Mg-vermiculite: *Amer. Mineral.* **51,** 1124–1143.

Tardy, Y. and Gac, J. Y. (1968) Minéraux argileux dans quelques sols et arènes des Vosges cristallines. Présence de vermiculite Al. Hypothèse de la formation des vermiculites et montmorillonites: *Bull. Serv. Cart. Géol. Als. Lorr.* **2,** 285–304.

Trescases, J. J. (1975) L'évolution géochimique des roches ultrabasiques en zone tropicale et la formation des gisements nickélifères de Nouvelle Calédonie: *Thèse Sc. Strasbourg, Mém. ORSTOM* **78,** 259 pp.

Van Oosterwyck-Gastuche, M. C. (1970) La structure de la chrysocolle: *C.R. Acad. Sci. Paris D,* **271,** 1837–1840.

Walker, G. F. (1949) The decomposition of biotite in the soil: *Mineral. Mag.* **28,** 693–703.

Wey, R., Le Dred, R., and Schoenfelder, J. (1966) Transformation d'un mica partiellement chloritisé en vermiculite par oxydation du fer(II): *Bull. Gr. Fr. Argiles* **12,** 107–114.

Wilson, M. J. (1966) The weathering of biotite in some Aberdeenshire soils: *Mineral. Mag.* **35,** 1080–1093.

Wilson, M. J. (1970) A study of weathering in a soil derived from a biotite-hornblende rock. I. Weathering of biotite: *Clay Miner.* **8,** 291–303.

(Received 3 August 1985; accepted 13 January 1986; Ms. 1510)